Electrochimica Acta 88 (2013) 373–383

Contents lists available at SciVerse ScienceDirect

Electrochimica Acta

journal homepage: www.elsevier.com/locate/electacta

Charged particle detection in the Pd/D system: CR-39 SSNTD vs. real-time measurement of charged particle stimulated Pd K shell X-rays

L.P. Forsley[a], P.A. Mosier-Boss[b,*], P.J. McDaniel[c], F.E. Gordon[d]

[a] JWK International Corp., Annandale, VA 22003, USA
[b] Research Laboratory of Electronics, Massachusetts Institute of Technology, Cambridge, MA 02139, USA
[c] University of New Mexico, Albuquerque, NM 87131, USA
[d] Navy Senior Executive Service (retired), San Diego, CA 92122, USA

ARTICLE INFO

Article history:
Received 18 July 2012
Received in revised form 20 October 2012
Accepted 20 October 2012
Available online 29 October 2012

Keywords:
Palladium
CR-39
X-rays
Charged particles

ABSTRACT

There have been a number of efforts to measure charged particle emissions in the Pd/D system. In general, two approaches have been employed. One approach was to indirectly detect charged particles by measuring Pd K-shell X-rays that should be created as charged particles traverse through the Pd lattice. The other approach utilized CR-39, a solid state nuclear track detector (SSNTD). With these detectors, a charged particle creates an ionization trail in the plastic that, upon etching, leaves a symmetric pit. The size, depth of penetration, and shape of the pits provides information about the mass, charge, energy, and direction of motion of the particles. While experiments done using CR-39 solid state nuclear track detectors have shown the presence of these charged particles, X-ray measurements of the Pd K-shell X-rays have not. The most significant difference between the two measurement techniques is that CR-39 is a constantly integrating detector and the X-ray measurements are done in real time. In this communication, this apparent discrepancy between the two charged particle measurement techniques is examined using known alpha sources.

Published by Elsevier Ltd.

1. Introduction

There have been a number of reports of charged particle detection in Pd/D systems using CR-39, a solid state nuclear track detector (SSNTD). Li et al. [1] were among the first to use CR-39 SSNTDs in experiments involving hydrogen/deuterium gas loading of palladium. In these experiments, palladium foil was in direct contact with the CR-39 detector and the temperature was cycled between room temperature and liquid nitrogen temperature. No tracks were observed for the hydrogen loading experiments. However, a large number of tracks in the CR-39 were obtained as a result of the deuterium gas loading experiments. The lack of tracks in the hydrogen gas experiments indicate that the observed pitting in the deuterium gas experiments was not due to chemical attack. Price et al. [2] conducted similar gas loading experiments as Li et al. [1], however they observed no tracks above background. Unlike Li et al., Price et al. had cleaned their Pd samples with aqua regia. When Li et al. [3] conducted deuterium gas loading experiments with Pd foils that had been cleaned with aqua regia, they too observed no tracks. Auger analysis of the foils showed that chlorine had penetrated inside the Pd to a depth of a few hundred angstroms. When chlorine gas was used to intentionally contaminate the Pd surface prior to conducting the deuterium gas loading experiment, no tracks were observed in the CR-39 detector. This was the first indication that surface treatments could suppress the nuclear effects occurring inside the Pd lattice.

Lipson et al. [4] and Roussetski [5] used CR-39 detectors to detect charged particles emitted from deuterated Au/Pd/PdO heterostructures. In these experiments, the heterostructures were electrochemically loaded with deuterium. Once loaded, the heterostructures were placed in contact with the CR-39 detectors and the temperature was cycled to induce desorption of deuterium. Lipson et al. [4] reported seeing tracks consistent with 2.5–3.0 MeV protons and 0.5–1.5 MeV tritons in the CR-39 detectors. Besides tracks consistent with DD reaction products, Roussetski [5] reported observing triple tracks in the detectors used in his experiments. These triple tracks are diagnostic of the carbon shattering reaction, $^{12}C(n,n')3\alpha$, typically caused by a $\geq$9.6 MeV neutron.

Oriani and Fisher [6] were the first to report on using CR-39 detectors in an electrolysis experiment. They placed the detectors above and below the anode so as to not impede uniform loading of the cathode with deuterium. During each run, control detectors were immersed in a bottled electrolyte solution. Track densities ranged between 59 and 541 tracks cm^{-2} for the control detectors and 156–3760 tracks cm^{-2} for detectors used in active cells. They concluded that the reactions responsible for the particles causing

* Corresponding author. Tel.: +1 858 576 6415.
E-mail address: pboss@san.rr.com (P.A. Mosier-Boss).

0013-4686/$ – see front matter. Published by Elsevier Ltd.
http://dx.doi.org/10.1016/j.electacta.2012.10.084

the tracks did not occur at the distant cathode but most likely occurred in the electrolyte very close to the plastic surface.

Lipson et al. [7,8] were the first to conduct *in situ* electrolysis experiments in which the Pd foil cathode was in direct contact with the CR-39 detector. Experiments were done in both heavy and light water. The observed tracks were concentrated in areas where the detector was in direct contact with the cathode indicating that the Pd foil was the source of the particles that caused the tracks. The distribution of tracks was inhomogeneous. This indicated that some sites in the Pd foil exhibit greater activity than others. Using Cu and Al spacers between the cathode and the detector and linear energy transfer (LET) curves, they were able to identify the particles as being 11–16 MeV alphas and ~1.7 MeV protons.

Mosier-Boss et al. [9–11] used CR-39 detectors in their Pd/D co-deposition experiments. The optical properties of the Pd/D co-deposition generated pits were consistent with those observed for tracks of a nuclear origin. Specifically the pits were dark and circular in shape and they exhibited bright centers when focusing the microscope optics deeper inside the pits. Track density was highest where the cathode had been in contact with the detector indicating that the source of the tracks was the cathode. The distribution of tracks along the cathode was inhomogeneous indicating that some Pd sites were more active than others. Control experiments showed that the tracks were not due to radioactive contamination of the cell components nor were they due to chemical or mechanical damage. Tracks were observed on both the front and the back surfaces of the detectors. The only particles that can traverse through 1 mm thick CR-39 detectors are ≥40 MeV alphas, ≥10 MeV protons, or neutrons. The size and shape of the tracks on the front side resembled those observed for alpha particles with energies between 1 and 2 MeV. Scanning of a CR-39 detector, used in a co-deposition experiment in which a 6 μm thick Mylar film separated the detector from the cathode, showed that the majority of the tracks had diameters between 0.3 and 4.3 μm [10]. Protons with energies >10 MeV would produce tracks with diameters in this size range [12]. Mosier-Boss et al. [13] also reported on seeing triple tracks in CR-39 detectors used in Pd/D co-deposition experiments. As discussed *vide supra*, such triple tracks are diagnostic of ≥9.6 MeV neutrons. It was also shown that the Pd/D co-deposition triple tracks were indistinguishable from DT neutron generated triple tracks [14].

Tanzella et al. [15] also conducted Pd/D co-deposition experiments using CR-39 detectors. They conducted both light and heavy water experiments as well as experiments in which 6 μm Mylar separated the cathode from the CR-39. In the experiments where the CR-39 was immersed in the electrolyte, a 60 μm thick polyethylene film separated the CR-39 from the cathode. In the heavy water experiments, they also saw pits in the CR-39 detectors that correlated with the placement of the cathode. Tracks were observed on both the front and back surfaces. Lipson and Roussetski [15] analyzed the CR-39 detectors using a sequential etching technique that they had developed, using alphas and protons of known energies, to differentiate charged particles and their energies. Using this process, they identified proton recoils due to 2.45 MeV neutrons, 3 MeV protons, 16 MeV alphas, and 12 MeV alphas in the CR-39 detectors used in heavy water experiments. No tracks above background were observed in the light water experiments. It should be noted that the sequential etching method has been used by other groups working with radioactive materials to identify and determine the energies of emitted charged particles [16–19].

Prior to the use of CR-39 to detect charged particles in these experiments, attempts were made to detect the Pd X-rays resulting from the refilling of the K shell electron orbits ionized by the passage of charged particles through the Pd lattice [20,21]. Both Bennington et al. [20] and Deakin et al. [21] used lithium drifted silicon, Si(Li), detectors to detect the X-ray emissions in real time. In these experiments, no X-rays above background were detected. The main difference between the two approaches to detect charged particles is that CR-39 is a constantly integrating detector while the measurement of the X-rays using a Si(Li) detector is done in real time. In this communication, the apparent discrepancy between the two approaches in detecting charged particles in the Pd/D system is examined.

2. Experimental

2.1. Real-time X-ray/gamma ray measurements

All X-ray/gamma ray measurements were made using a cryogenically-cooled 18% HPGe detector with a Be window (Ortec). The detector head and samples were placed in a Pb cave. To reduce the Pb fluorescence, the inside of the cave was lined with Sn foil. Cu foil, between the Sn foil and the sample, was used to eliminate the Sn fluorescence. Sample orientation inside the cave is discussed *vide infra*. Compared to a Si(Li) detector, the HPGe detector used in these experiments is more sensitive to 21.1 keV Pd K shell X-rays.

All manipulations of spectral data were done using GRAMS/A17 (ThermoGalactic). This software package is used to subtract spectra interactively as well as integrate peak areas and measure peak intensities.

2.2. Silicon barrier detector measurements

Experiments were conducted stacking layers of 6 μm thick Mylar sheets on top of one another between the CR-39 detector and an ^{241}Am source. To determine the energies of the alpha particles getting through the Mylar, a silicon barrier detector (AMETEK model TR-SNA-300-100) was used. A ~0.5 mm wide slit was placed between the detector and the ^{241}Am source to block particles emitted at oblique angles. This allows particles that are approximately perpendicular to the plane of the Si barrier detector to reach the detector thereby reducing the backscatter. The slit used in these experiments was made from 100 μm thick acrylic plastic.

2.3. Etching of CR-39 and analysis of the etched detectors

The CR-39 detector was exposed to a ^{210}Po source for 3 min. Afterwards the detector was etched in an aqueous 6.5 N sodium hydroxide solution at 65–72 °C for 6 h. After etching, the detector was rinsed in water, vinegar, and again in water. Microscopic examination of the etched CR-39 detector was done using an Eclipse E600 epifluorescent microscope (Nikon) and CoolSnap HQ CCD camera (Photometrics). A magnification of 1000× was used. The software used to obtain the images was MetaVue (MDS Analytical Technologies).

3. Results and discussion

3.1. Overview of the 1989 X-ray measurements using Si(Li) detectors

The cell used by Deakin et al. [21] was constructed of Pyrex glass with a thin blown Pyrex window. The Pd foil cathode was 50 μm thick and had an area of 1 cm^2. The cathode was pressed against the thin Pyrex window. The X-ray detector was placed on the other side of the Pyrex window. The ability of the detector to register K shell X-rays from the Pd cathode was checked by fluorescing the electrode using Ba X-rays after the cell had been filled with electrolyte. They observed that room background radiation caused the Pd cathode to fluoresce and a line due to Pd K shell X-rays was present as an artifact in the background. After 333 h of electrolysis

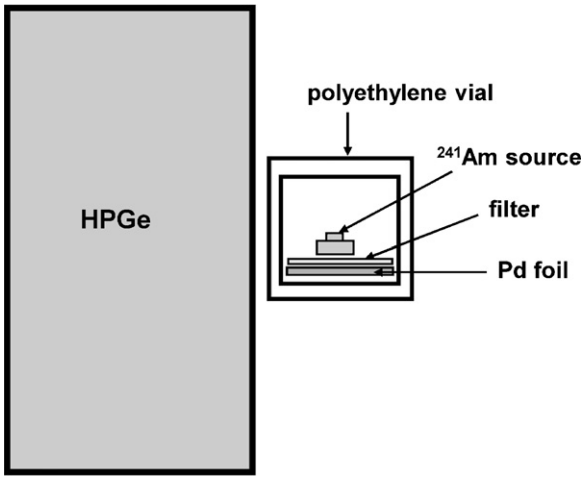

Fig. 1. Schematic of the experimental configuration used in the ^{241}Am stimulation experiments. The ^{241}Am source came from a smoke detector. Filters used in these experiments were either 18 μm Mylar or 560 μm Cu foil. The Pd foil was 25 μm thick with an area of 0.38 cm^2. The polyethylene vial was placed against the Be window of the HPGe. All measurements were conducted inside a Pb cave lined with Sn and Cu.

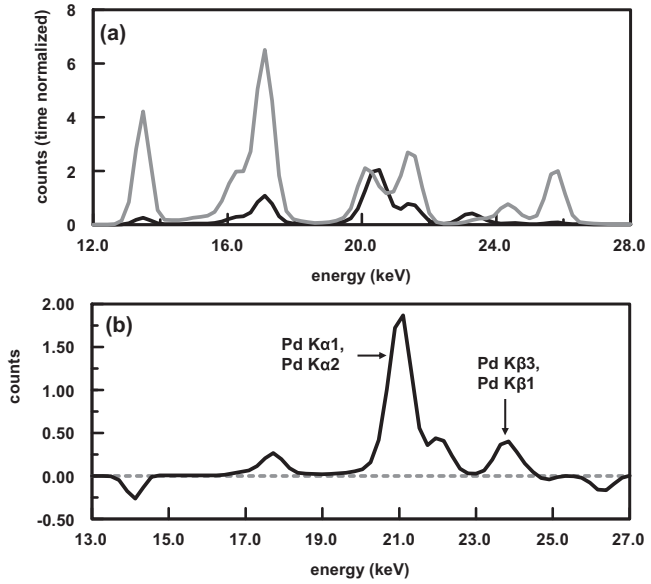

Fig. 2. (a) Time normalized X-ray spectra in the Pd K shell X-ray region where the gray line was obtained for the ^{241}Am source and the black line was obtained for the ^{241}Am source in contact with 25 μm thick Pd foil. (b) X-ray spectrum of the Pd foil in which the contributions of the ^{241}Am source are subtracted out. The Pd Kα and Pd Kβ lines are identified.

at a current density of 300 mA cm^{-2}, they saw no X-ray emissions above background.

Bennington et al. [20] used an electrolytic cell with a thin Mylar window. The Pd disc cathode was 1.5 mm thick and 20 mm in diameter. The gap between the Pd cathode and Mylar window was less than 1 mm. A peristaltic pump was used to pump the electrolyte past the electrodes to prevent the trapping of gas bubbles between the cathode and the Mylar window. The Si(Li) detector was placed on the other side of the window so that only a small amount of electrolyte and Mylar separated it from the possible source. Absorption of the Pd K shell X-rays by water, Mylar, and air was estimated to be 6%. A calibration run was performed with a 150 nCi ^{241}Am α source placed against the rear of a 0.1 mm thick Pd foil that was in contact with the Si(Li) detector. Unlike Deakin et al. [21], no Pd K shell X-ray lines were present in the background spectra. Several electrolysis experiments were performed using current densities of about 150 mA cm^{-2}. No X-rays above background were observed.

3.2. The use of Americium-241 to stimulate X-ray emissions in Pd

A schematic of the experimental configuration is shown in Fig. 1. The ^{241}Am source used in these experiments came from a smoke detector. As such the ~1 μCi ^{241}Am disc is mounted inside a metal housing and has either a thin Au or Al film over it. Fig. 2a shows X-ray spectra in the Pd X-ray region obtained for the ^{241}Am source by itself and in contact with a 25 μm thick Pd foil that has an area of 0.38 cm^2. X-ray lines are seen in the spectrum of the ^{241}Am source. These lines could possibly be due to X-rays from the constituents of the metal housing that are stimulated by the emissions of the ^{241}Am source. These lines decrease when the Pd foil is placed in contact with the ^{241}Am source. Fig. 2b shows the spectrum of the Pd foil in which the contributions of the ^{241}Am source are subtracted out. The Pd Kα and Pd Kβ lines are identified.

The Pd deposit formed as a result of Pd/D co-deposition has a cauliflower-like morphology that traps pockets of water. Consequently, the charged particles have to traverse a film of water before they reach the CR-39 detector [10]. As was discussed *vide supra*, the size and shape of the tracks on the front side of the CR-39 detector used in a Pd/D co-deposition experiment resemble those observed for alpha particles with energies between 1 and 2 MeV. It was therefore of interest to determine the effect of alpha particle energy on the magnitude of the Pd K-shell X-rays. To vary the energy of the alpha particles, sheets of Mylar were placed between the ^{241}Am source and the Pd foil. Fig. 3a shows the linear energy transfer (LET) curve for alphas as a function of Mylar thickness. This LET curve was calculated using the SRIM-2003.26 code of Ziegler and Biersack [22]. The LET curve indicates that 6, 12, and 18 μm of Mylar will decrease the energy of the alphas by ~1.2, 2.7, and 3.6 MeV respectively. This was verified by measurements using a silicon surface barrier (SSB) detector, a charged particle detector that does not respond to gamma or X-rays. Fig. 3b summarizes results obtained by placing 6, 12, and 18 μm of Mylar between the ^{241}Am source and the Pd foil. Besides decreasing the energy of the alphas, the Mylar also causes a decrease in the number of alpha particles that can get through to reach the SSB detector.

If the alpha particles emitted by the ^{241}Am source are responsible for stimulating the Pd K-shell X-rays, a corresponding decrease in the intensity of the Pd K shell X-rays is expected when Mylar is placed between the ^{241}Am source and Pd foil. Looking at Fig. 3b, 18 μm of Mylar should result in a 75% decrease in intensity of the Pd K shell X-rays. Fig. 3c shows X-ray spectra of the ^{241}Am source and Pd foil in the presence and absence of 18 μm of Mylar. No decrease in X-ray intensity was observed, indicating that something else is primarily responsible for stimulating the Pd K shell X-rays.

Besides emitting alphas, ^{241}Am emits a gamma-ray at 59.54 keV [23]. Fig. 3d shows spectra of the ^{241}Am gamma-ray. When the ^{241}Am source is in contact with the Pd foil, it can be seen that the intensity of the gamma ray decreases. Fig. 3d also shows that the 18 μm of Mylar has no additional affect on the intensity of the ^{241}Am gamma-ray. These results suggest that the Pd foil is absorbing the ^{241}Am gamma ray. It is the absorption of this ^{241}Am gamma ray by the Pd foil that stimulates the Pd K shell X-ray emissions. It is probably this gamma-ray, and not the ^{241}Am α particles, that stimulates the emissions observed for the housing of the ^{241}Am source, Fig. 2a.

To further verify that the ^{241}Am gamma ray is stimulating the Pd K shell X-rays, a 560 μm thick Cu foil was placed between the ^{241}Am source and Pd foil. The Cu foil will block all ^{241}Am alpha particles but not the ^{241}Am gamma-ray at 59.54 keV. Fig. 4a (gray line) shows an X-ray spectrum in the Pd X-ray region obtained for the

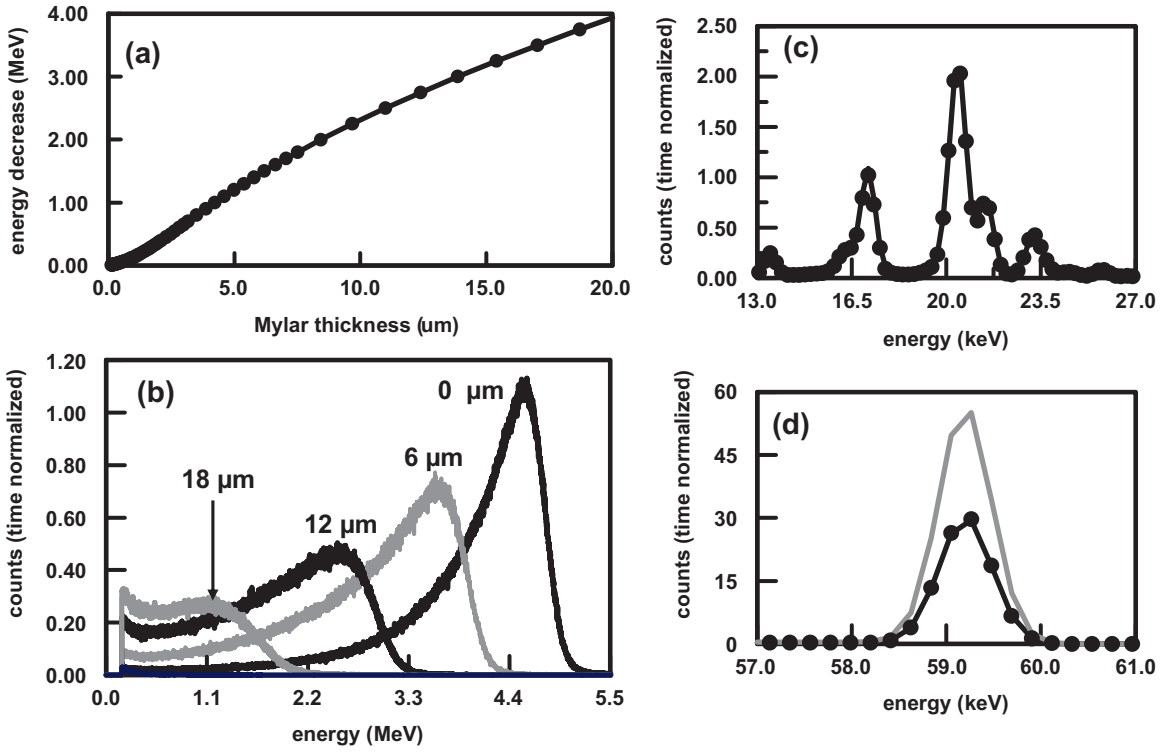

Fig. 3. (a) LET curve showing the expected decrease in energy of alpha particles as a function on thickness of the Mylar film. (b) Alpha spectra obtained by placing 0, 6, 12, and 18 μm of Mylar between a silicon surface barrier (SSB) detector and the ^{241}Am source. The spectra have been time normalized. (c) X-ray spectra in the Pd K shell X-ray region obtained for a 25 μm thick Pd foil exposed to a ^{241}Am source in the presence (●) and absence (black line) of 18 μm of Mylar between the Pd foil and the ^{241}Am source. (d) Spectra of the ^{241}Am gamma-ray region where the gray line is that of the ^{241}Am source, the black line was obtained by placing the ^{241}Am source in direct contact with the 25 μm thick Pd foil, and (●) was obtained by placing 18 μm of Mylar between the ^{241}Am source and the 25 μm thick Pd foil.

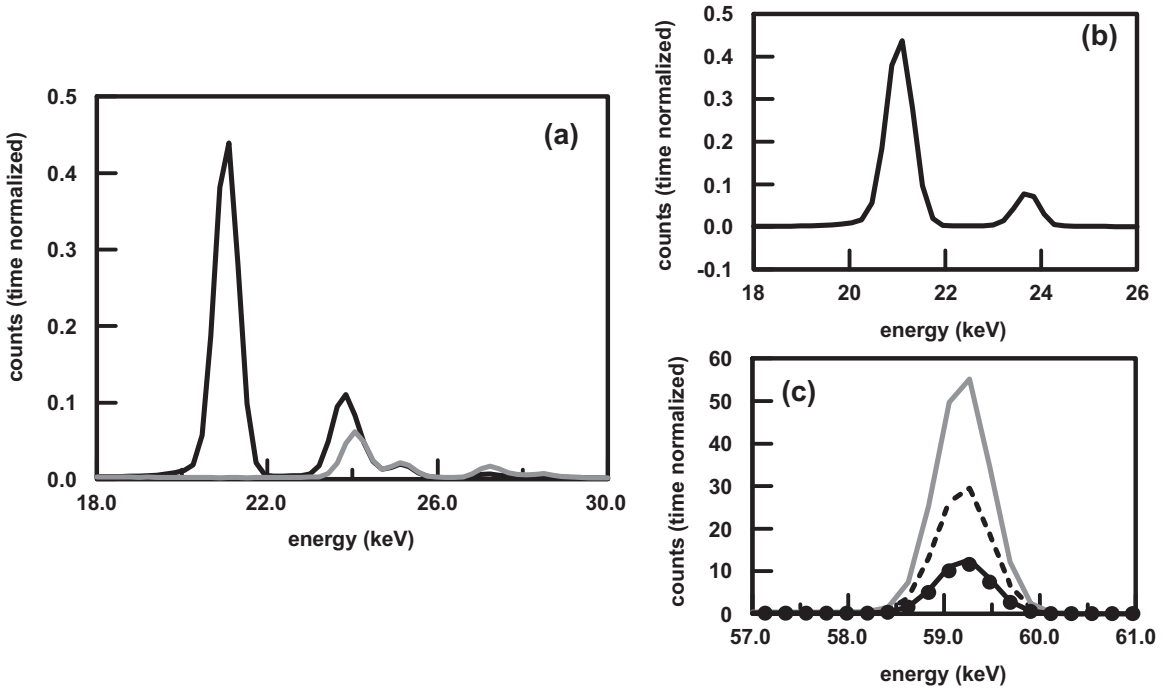

Fig. 4. (a) Time-normalized X-ray spectra in the Pd K shell X-ray region where the gray line was obtained with the ^{241}Am source in direct contact with the 560 μm thick Cu foil and the black line was obtained by placing the 560 μm thick Cu foil between the ^{241}Am source and the 25 μm thick Pd foil. (b) X-ray spectrum of the Pd foil in which the contributions of the ^{241}Am-Cu emissions have been subtracted out. The large line at 21.1 keV is due to the Pd Kα X-rays and the smaller line at 23.85 keV is assigned to the Pd Kβ X-rays. (c) Spectra of the ^{241}Am gamma-ray region where the gray line is that of the ^{241}Am source, the black dashed line was obtained by placing the ^{241}Am source in direct contact with the 25 μm thick Pd foil, the black solid line was obtained by placing the ^{241}Am source in direct contact with the 560 μm thick Cu foil, and (●) was obtained by placing the 560 μm Cu foil between the ^{241}Am source and the 25 μm thick Pd foil.

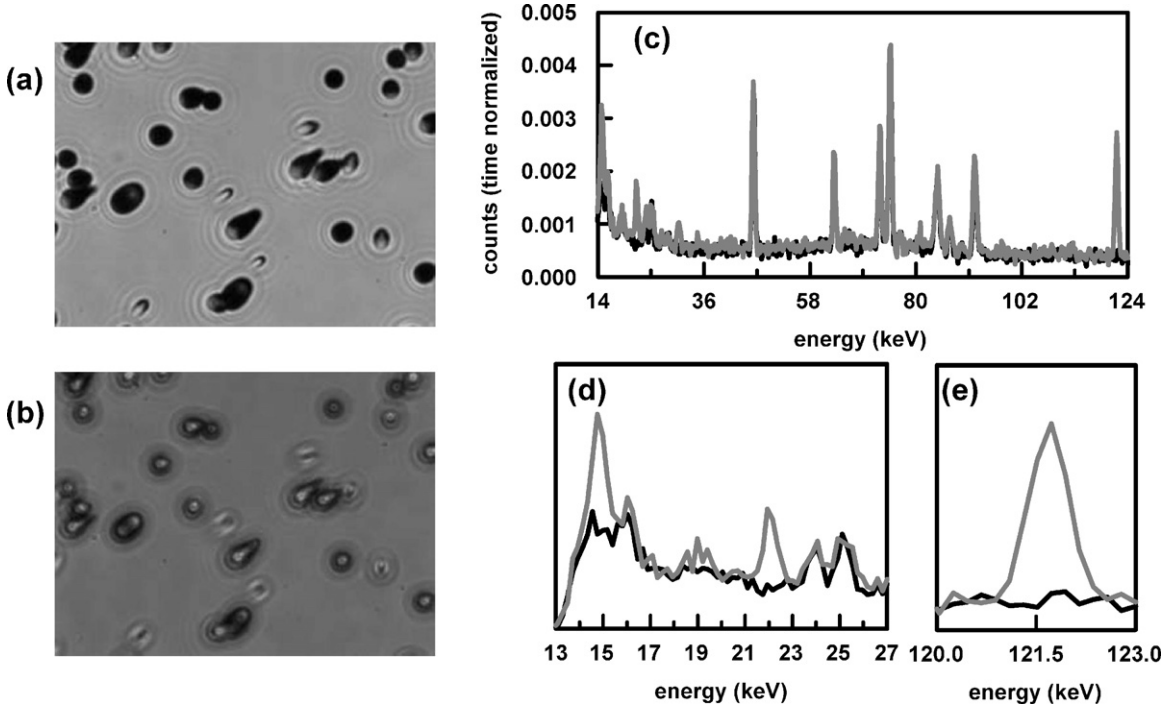

Fig. 5. Photomicrographs of alpha tracks, at 1000× magnification, obtained by exposing CR-39 to a 0.1 μCi ^{210}Po source for 3 min where (a) was obtained by focusing the microscope optics onto the surface of the detector and (b) was an overlay of two images taken at the surface and bottom of the pits. Time-normalized, X-ray spectra obtained for the background (black line) and the 0.1 μCi ^{210}Po source (gray line) for the spectral regions (c) 14–124 keV, (d) 13–27 keV, and (e) 120–123 keV. The spectrum of the ^{210}Po source was obtained by placing the source in direct contact with the Be window of the HPGe detector.

^{241}Am source in contact with the 560 μm thick Cu foil. Comparing the spectrum with that of the ^{241}Am source itself, gray line Fig. 2a, it can be seen that the Cu foil absorbs the majority of the gamma-ray induced emissions due to the source housing. The spectrum obtained by placing the 560 μm thick Cu foil between the ^{241}Am source and Pd foil is also shown in Fig. 4a (black line). The observed spectrum is cleaner than that observed for ^{241}Am source in direct contact with the Pd foil, black line Fig. 2a. Fig. 4b shows the spectrum of the Pd foil in which the contributions of the ^{241}Am source and Cu foil are subtracted out. This difference spectrum shows Pd Kα X-rays at 21.1 keV and Pd Kβ at 23.85 keV. Fig. 4c shows the spectra of ^{241}Am gamma ray of the ^{241}Am source alone and in contact with the Pd foil, Cu foil, and both Pd and Cu foils. These spectra show the absorption of the ^{241}Am gamma ray when the Pd and/or Cu foils are exposed to the source. Because the Cu foil is thicker, it attenuates the signal more.

3.3. The use of Polonium-210 to stimulate X-ray emissions in Pd

The experimental results obtained using a ^{241}Am source showed that the gamma-ray at 59.54 keV was primarily responsible for stimulating the Pd K shell X-ray emissions that were measured and not the alpha particles. This is due to the fact that gamma rays are much more penetrating than alphas particles. To evaluate the stimulation of X-rays by alpha particles, a source that decays purely by alpha emission, ^{210}Po, was obtained. The source, which was mounted in a plastic housing, had an initial activity of 0.1 μCi. Fig. 5a and b shows alpha tracks in CR-39 obtained by exposing the detector to the ^{210}Po source for 3 min. The microphotograph of the alpha tracks shown in Fig. 5a was obtained by focusing the microscope optics on the surface of the detector while Fig. 5b was obtained by overlaying two images taken on the surface of the detector and the bottom of the pits. The observed number of tracks is consistent with a 0.1 μCi alpha source. From the image taken with the microscope optics focused on the surface of the detector, it can be seen that the tracks are dark in color and either circular or elliptical in shape. Focusing inside the tracks, bright centers are observed inside the pits. The bright centers indicate that the bottoms of the tracks are rounded [24]. These features are diagnostic of nuclear-generated tracks.

A gamma-ray spectrum of the ^{210}Po source was obtained by placing the source inside the lead cave and pressed against the Be window of the HPGe detector. Fig. 5c–e shows the spectra obtained for the lead cave with and without the ^{210}Po source. The spectra were time normalized. From the spectra, it can be seen that three new gamma/X-ray lines at 14.8, 21.9, and 121.7 keV are present in the ^{210}Po source spectrum. As ^{210}Po is a pure alpha emitter, these new lines cannot be due to ^{210}Po. Compared to the ^{241}Am gamma line at 59.54 keV, Fig. 3d, the three gamma/X-ray lines seen in Fig. 5d and e are very small and are attributed to gamma/X-ray emitting contaminant(s) in the ^{210}Po source.

Experiments were conducted placing 25 μm thick Pd foil in contact with the ^{210}Po source. The area of the Pd foil was 16.1 cm^2. Spectra were obtained using both 'facing' and 'not-facing' configurations, shown in Fig. 6. When the Pd and ^{210}Po source were not directly facing the Be window of the HPGe detector, no lines due to the Pd or to the contaminant in the ^{210}Po source were observed in the spectrum. However, when the Pd foil and ^{210}Po source were facing the Be window of the HPGe detector, the Pd Kα line at 21.1 keV was observed as was the 21.9 keV line due to the contaminant in the ^{210}Po source. The significance of orientation on the observation of the Pd K shell lines in Pd/D experiments will be discussed *vide infra*.

While the presence of the contaminant in the ^{210}Po source was unexpected, it did present an opportunity to separate and quantify the alpha/gamma contributions in stimulating the Pd K shell X-rays. This was not possible using the ^{241}Am source due to the intensity of the gamma ray. To isolate and quantify the alpha/gamma contributions, a 100 μm thick acrylic sheet was placed between the Pd foil and the ^{210}Po source. The acrylic sheet

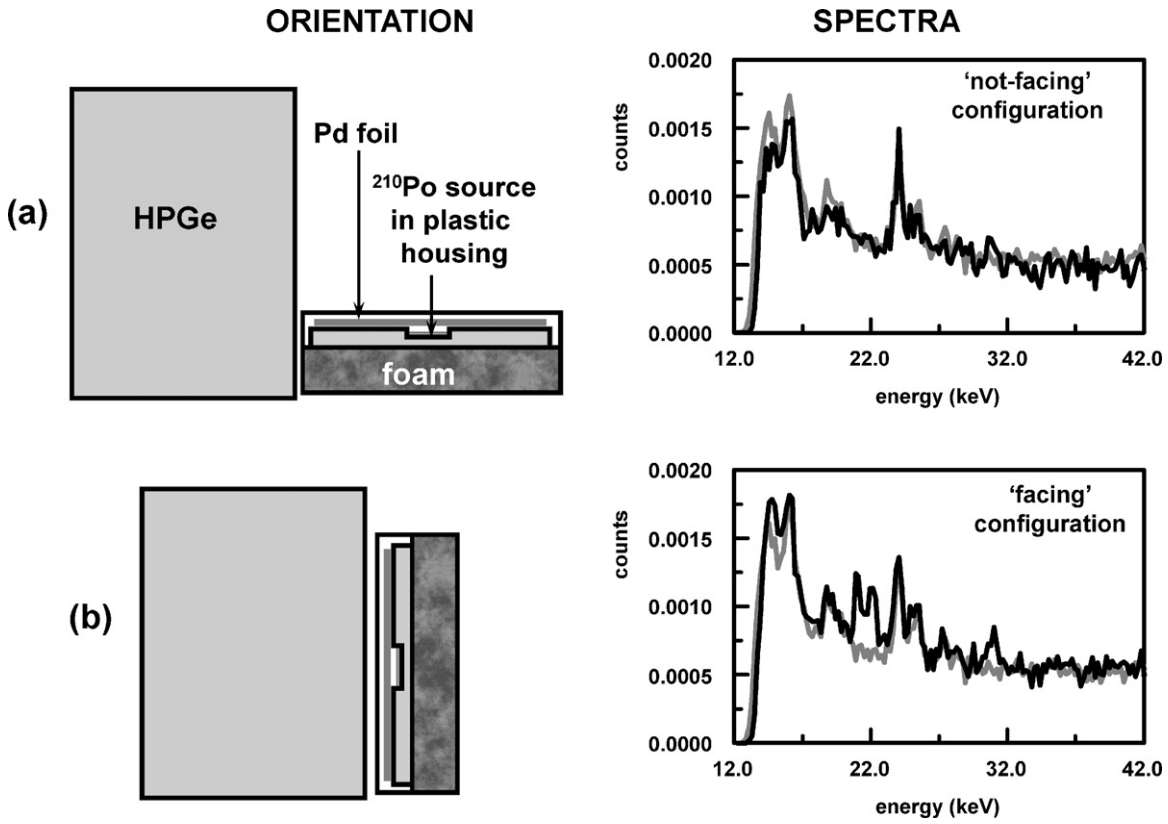

Fig. 6. Left hand side shows schematics of how the Pd and ^{210}Po source were oriented relative to the face of the Be window of the HPGE where (a) is the 'not-facing' configuration and (b) is the 'facing' configuration. Right hand side shows the time-normalized spectra obtained where the gray line is due to the lead cave background and the black line is due to the Pd-^{210}Po source. The configuration the spectra were obtained is indicated. All measurements were conducted inside a Pb cave lined with Sn and Cu.

will block the alphas from the ^{210}Po but not the gamma/X-rays from the contaminant(s). The time normalized results are summarized in Fig. 7. All spectra were obtained using the 'facing' configuration. Light gray blocks indicate the regions of the gamma lines due to an unknown contaminant in the ^{210}Po source and the darker gray box indicates the region of the Pd Kα line.

Fig. 7a shows the spectrum obtained for the Pd foil. The foil was 25 μm thick and had an area of 16.1 cm^2. A very small peak due to the Pd Kα shell X-rays was observed in the spectrum. The foil used in the ^{210}Po source experiments had 42 times more surface area than the foil used in the ^{241}Am experiments discussed *vide supra*. For the smaller foil used in the ^{241}Am experiments, the Pd Kα X-ray lines were not observed. The lead cave X-rays between 36 and 102 keV, Fig. 5c, are probably responsible for stimulating the Pd K shell X-rays resulting in the peak seen in Fig. 7a. The spectrum obtained for the ^{210}Po source is shown in Fig. 7b. Only noise is observed in the region of the Pd K shell X-rays. Two gamma/X-rays at 14.8 and 21.9 keV, due to unknown contaminant(s), were observed in the spectrum.

The spectrum obtained when the Pd foil in contact with the ^{210}Po source is shown in Fig. 7c. The line due to the Pd K shell X-rays is more prominent than that observed in the background. When a 100 μm thick acrylic sheet is placed between the Pd foil and the ^{210}Po source, a decrease in the line due to the Pd K shell X-rays is observed, Fig. 7d. Compared to the ^{210}Po source spectrum, Fig. 7b, a decrease is observed in the intensities of the unknown contaminant gamma rays at 14.8 and 21.9 keV. These spectra indicate that both the ^{210}Po α particles and the γ-rays from the unknown contaminant(s) are stimulating the emission of Pd K shell X-rays. Table 1 summarizes the measured intensities of the Pd Kα lines in Fig. 7 as well as the sources of the stimulation. It is assumed that the background, ^{210}Po α-particle, and unknown contaminant γ-ray stimulations contribute additively to the Pd Kα emissions of the Pd-^{210}Po sample, Fig. 7c. With this assumption, the estimated contributions of each source in stimulating the Pd Kα emissions are 35.2% due to background, 44.4% due to the ^{210}Po α-particles, and 20.4% due to the unknown contaminant(s) gamma/X-rays.

3.4. Implications to the CR-39 detection results obtained for Pd/D experiments

The results of the ^{210}Po–Pd experiments discussed *vide supra* can be used to determine whether or not Pd K shell X-rays would have been observed in the CR-39 experiments [1,3–11,13–15]. The gas loading experiments done by Li et al. [1,3] and Price et al. [2] were done in stainless steel cells. The stainless steel would have absorbed any Pd K shell X-rays. In order to see these X-rays, the X-ray detector would have to be placed inside the stainless steel vessel and cycled between room and liquid nitrogen (−196 °C) temperatures. Currently, Hamamatsu offers compact, X-ray detectors comprised of a Si photodiode coupled to a scintillator that are ideal for the detection of X-rays below 100 keV [25]. Although these X-ray detectors

Table 1
Analysis of the Pd Kα line shown in the spectra in Fig. 7.

Sample[a]	Intensity of Pd Kα line[b]	Cause of stimulation[c]
^{210}Po source	0.00	None
Pd foil	1.9×10^{-4}	bkg
^{210}Po–Pd foil	5.4×10^{-4}	bkg + α + γ
^{210}Po-100 μm acrylic-Pd foil	3.0×10^{-4}	bkg + γ

[a] All samples were measured in a Pb cave that was lined with Sn and Cu foil.
[b] Spectra have been time normalized. Pd Kα line is shown in Fig. 7.
[c] Bkg = background stimulation, α = alphas from ^{210}Po source; γ = gamma rays from the unknown contaminant(s) in the ^{210}Po source.

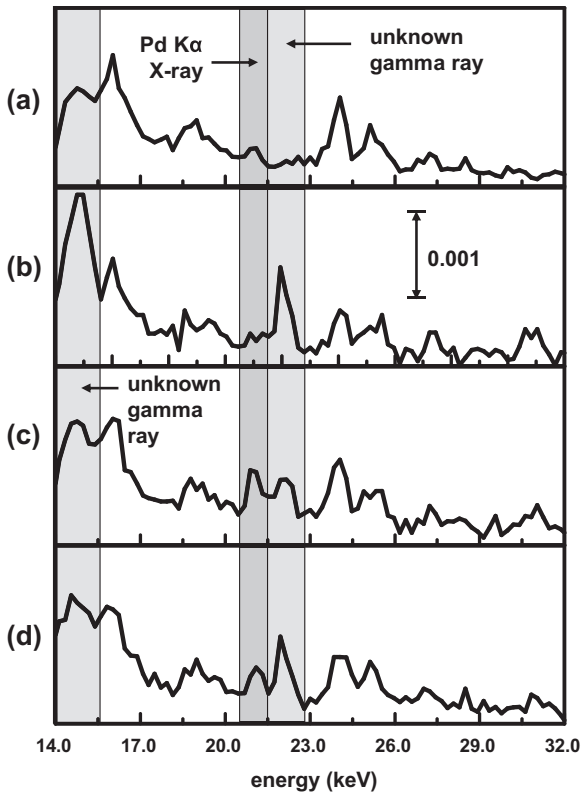

Fig. 7. Time-normalized X-ray spectra in the Pd K shell X-ray region obtained using the 'facing' configuration where (a) is the 25 μm thick, 16.1 cm^2 area Pd foil, (b) is the ^{210}Po source, (c) is the Pd foil in direct contact with the ^{210}Po source, and (d) has a 100 μm thick acrylic film between the Pd foil and the ^{210}Po source. The light gray box indicates the regions of the gamma lines at 14.8 and 21.9 keV due to unknown contaminant(s) in the ^{210}Po source. The darker gray box indicates the region of the Pd Kα lines. All spectra were measured in a lead cave lined with Sn and Cu.

would be small enough to be placed inside the stainless steel vessel, their operating temperature range is between −10 and 60 °C. Consequently any charged particle emissions that occurred between −10 and −196 °C would not be registered by these X-ray detectors. This would not be true for a SSNTD such as CR-39. Therefore, it would not have been possible to detect the presence of charged particles in the gas-loading experiments by Pd K shell X-ray emissions.

The presence of a line due to the Pd K shell X-rays in the background, Fig. 7a, is in agreement with the work of Deaken et al. [21]. However, Bennington et al. [20], who used much thicker Pd cathodes in their experiments, did not observe a line due to the Pd K shell X-rays in their background. There are two possible explanations for these results. One is that the Si(Li) detector used by Bennington et al. was not as sensitive as the X-ray detector used by either Deaken et al. or the HPGe detector used in this effort. The other explanation is that the thicker Pd foil used by Bennington et al. absorbed the Pd K shell X-rays stimulated by the background. The more likely cause is the later. The formula used to calculate the percentage of X-rays absorbed in a material is

$$A = 100[1 - \exp(-\mu\rho x)] \quad (1)$$

where A is the percentage of X-rays absorbed, μ is the mass absorption coefficient of X-rays at a given energy, ρ is the density of the material, and x is the thickness of the material [26]. For a high Z material like Pd, the absorption coefficient is dominated by photoabsorption [27]. The photoabsorption coefficient of Pd at an X-ray energy of 21.1 keV is 13.61 $cm^2\,g^{-1}$ and the density of Pd is 12.0 $g\,cm^{-3}$ [28]. Using these values, the plot of % X-rays absorbed as a function of Pd thickness was calculated, Fig. 8a. The 50 μm thick foil used by Deaken et al. would absorb 55.8% of the X-rays while that used by Bennington (1.5 mm thick) would absorb 100%. In contrast, the foil used in our experiments was 25 μm thick and would have absorbed 33.5% of the X-rays. Based upon these calculations, the thickness of the Pd foil used in the Bennington et al. experiment greatly impacted their ability to see any Pd X-ray emissions during an electrolysis experiment.

Table 2
Measured peak areas of the Pd Kα line shown in the time normalized spectra in Fig. 9a and b.

Sample[a]	Area of Pd Kα line	Cause of stimulation[b,c]
Pd foil	9.22×10^{-5}	bkg
^{210}Po-100 μm acrylic-Pd foil	1.453×10^{-4}	bkg + γ

[a] All samples were measured in a Pb cave that was lined with Sn and Cu foil.
[b] Bkg = background stimulation, γ = gamma rays from the unknown contaminant(s) in the ^{210}Po source.
[c] The peak area resulting from stimulation by the unknown γ source is 5.31×10^{-5}.

Lipson et al. conducted electrolysis experiments using 8–300 μm thick Pd foils [8] or 2000–4000 Å thick Pd films [7] as cathodes. For the 8–300 μm thick Pd foils, the % X-rays absorbed was between 12.2 and 99.3%, as calculated using Eq. (1). The % X-rays absorbed by the Pd films was less than 1%. In these electrolysis experiments, the cathode was in the center and the anode surrounded it. A significant amount of water was present between the cathode and the cell wall, which was probably borosilicate glass. This configuration assured uniform loading of the Pd cathode with deuterium. However, the water and cell wall would also absorb any Pd K shell X-rays produced during the course of the experiment. For low Z materials, like H and O, Compton (in-elastic) scattering becomes significant at the higher X-ray energies and the absorption coefficient is no longer dominated by photoabsorption [27]. However, there is code available that calculates the % attenuation of X-rays as a function of X-ray energy and target length for a limited number of materials [29]. Using this code, the % attenuation of the 21.1 keV X-rays as a function of borosilicate glass and water thickness was calculated. The results are summarized in Fig. 8b and c, respectively. Lipson et al. did not provide any dimensions on their cells. However, estimates can be made. Typically borosilicate glass walls used in electrochemical cells are 1 mm thick, which would attenuate the X-rays by 36%, Fig. 8b. Typically electrochemical cells have inner diameters between 20 and 40 mm. With the cathode in the center, the water thickness the X-rays have to penetrate would be between 10 and 20 mm, which would attenuate the X-rays by 51.9–83.9%, Fig. 8c. The total attenuation through the water and borosilicate glass is estimated to be between 87.9 and 100%. Taking into account the attenuation of the 21.1 keV X-rays by the cell components, it is unlikely that any Pd K shell X-rays stimulated by charged particles would have been observed. Furthermore, Lipson et al. observed a relatively low number of tracks in their CR-39 detectors. In one electrolysis experiment involving 2000 Å of Pd on glass that ran for 48 h, Lipson et al. [7] identified 173 alpha and proton tracks above background. The measured rates of production were $(9.6 \pm 1.0) \times 10^{-4}\,\alpha\,s^{-1}$ and $(57.2 \pm 4.1) \times 10^{-4}\,p\,s^{-1}$, both in 4π steradian. It can be shown that such a low production rate of charged particles would not stimulate a detectable amount of Pd K shell X-rays. Fig. 9a and b shows the time normalized spectra measured, in the Pb cave, for the Pd foil and for the experiment in which the 100 μm thick acrylic sheet was placed between the Pd foil and the ^{210}Po source. In both spectra, the peak due to the Pd K shell X-rays is shown in gray. The measured peak areas are tabulated in Table 2. From the data, the peak area, resulting from stimulation by the γ-rays from the unknown contaminant(s) in the ^{210}Po source, is measured to be 5.31×10^{-5}. In Table 3, the calculated peak areas of the Pd K shell X-ray line resulting from

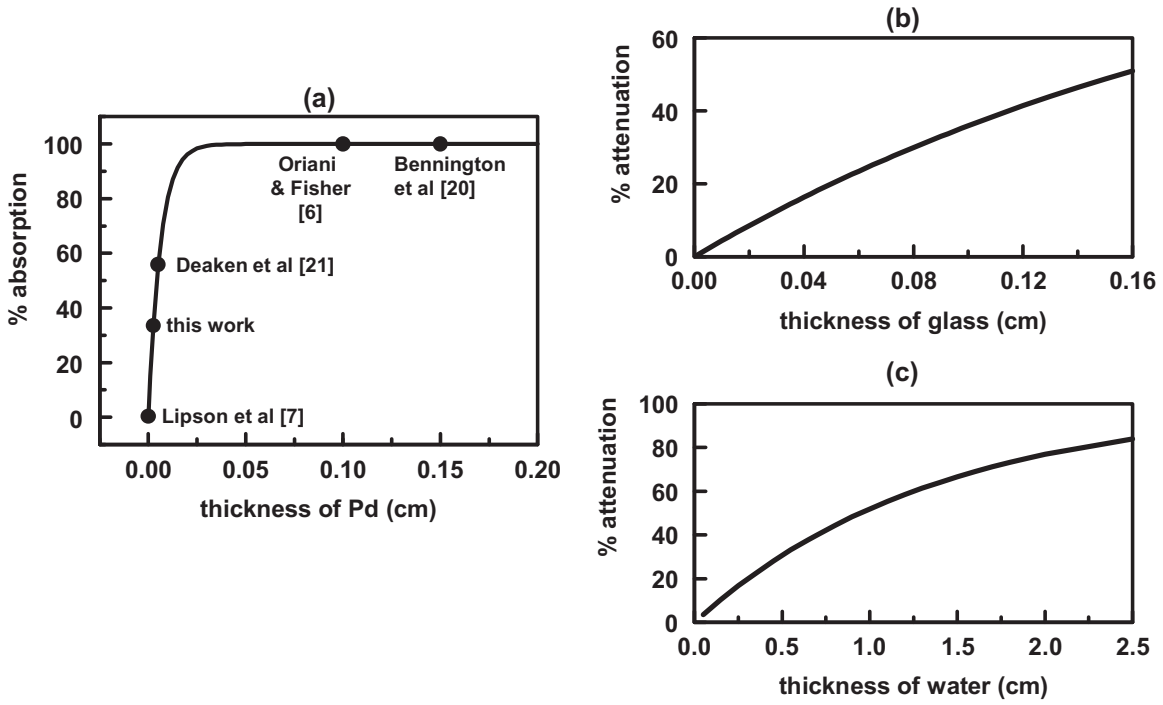

Fig. 8. (a) Plot of the % absorption of Pd X-rays as a function of Pd thickness. The thicknesses of the Pd cathodes used by Oriani [6], the 2000–4000 Å films used by Lipson et al. [7], Bennington et al. [20], Deaken et al. [21] and the authors of this paper are indicated. (b) Plot of % attenuation of Pd X-rays as a function of borosilicate glass thickness. (c) Plot of % attenuation of Pd X-rays as a function of water thickness.

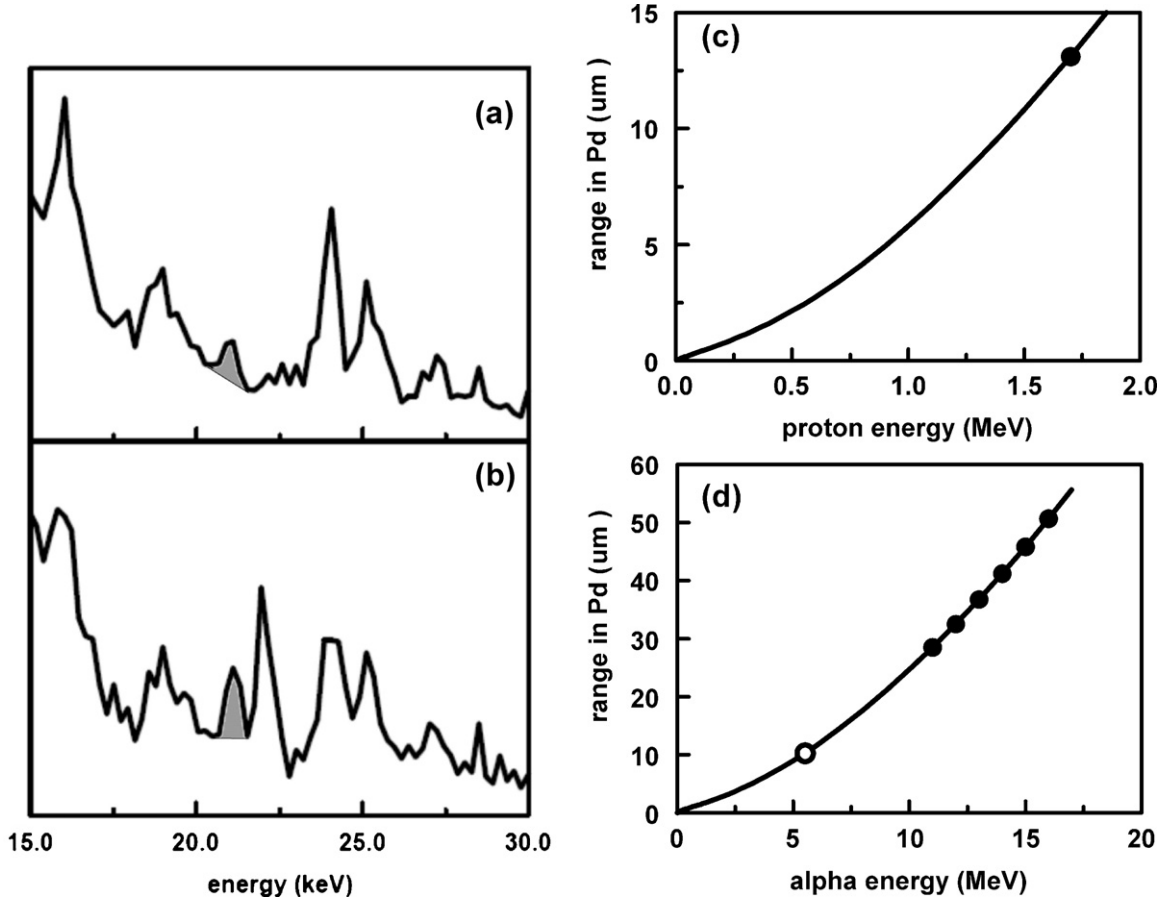

Fig. 9. Time normalized spectra obtained for (a) the 25 μm thick, 16.1 cm^2 area Pd foil and (b) the 100 μm thick acrylic film between the Pd foil and the ^{210}Po source. The line due to the Pd K-shell X-ray is shaded in gray. Peak areas are tabulated in Table 2. (c) LET curve calculated for energetic protons in Pd where ● indicates the 1.7 MeV proton. (d) LET curve for energetic alphas in Pd where ● indicates the 11–16 MeV alphas and ○ the 5.3 MeV ^{210}Po alpha.

Table 3
Calculating the peak area of the Pd Kα line caused by α stimulation using the spectral data shown in Figs. 7, 9a and b.

Stimulant	Contribution (%)	Calculated peak area
bkg[a]	35.2	9.22×10^{-5}
γ	20.4	5.34×10^{-5}
α[b]	44.4	1.163×10^{-4}

[a] This is the measured peak area for the Pd Kα line obtained by background stimulation.
[b] The ^{210}Po has an α activity of 0.1 μCi. This activity is equivalent to 3700 decays s^{-1}. Since the spectra are time normalized, the calculated peak area is due to stimulation by 3700 α particles.

γ and α stimulation are tabulated. The calculated peak area due to γ stimulation agrees well with the measured value. A 0.1 μCi ^{210}Po α source will have 3700 decays s^{-1}. For the time normalized spectra, this means that 3700 α particles will result in a Pd K shell X-ray line with a peak area of 1.163×10^{-4}. However, this peak area is for ^{210}Po whose alphas have an energy of 5.3 MeV. LET calculations indicate that the range of these 5.3 MeV alphas in Pd is 9.76 μm. Lipson et al. identified their particles as 1.7 MeV protons and 11–16 MeV alphas. LET curves for protons and alphas are shown in Fig. 9c and d, respectively. These plots indicate that the 1.7 MeV protons and 11–16 MeV alphas have longer ranges than the 5.3 MeV ^{210}Po alphas. Consequently, they will stimulate more X-rays than the ^{210}Po alphas as they traverse through the Pd lattice. Table 4 summarizes the calculations done to estimate the expected Pd K shell X-ray peak areas resulting from the passage of 1.7 MeV protons, 11 MeV alphas, and 16 MeV alphas through the Pd lattice. For the measured production rates of 9.6×10^{-4} 1.7 MeV protons and 57.2×10^{-4} 16 MeV alphas, as observed by Lipson et al. [7], the estimated increases in peak area resulting from the charged particle stimulation are 4.05×10^{-11}, 5.24×10^{-10}, and 1.03×10^{-9}, respectively. These increases would be too small to see in a measured spectrum.

In the experiments done by Oriani and Fisher [6], the CR-39 detectors were placed above and below the anode. As charged particles cannot travel far in water, the tracks observed in the CR-39 detectors are not attributable to charged particles. Although they are not using CR-39 to directly measure charged particles, it is unlikely that Pd K shell X-rays would have been detected in the electrolysis experiments done by Oriani and Fisher. As shown in Fig. 6, the orientation of the cathode relative to the window of the detector determines whether or not the Pd X-ray emissions will be observed. In the electrolysis experiments done by Oriani and Fisher, the cathode was in the 'not-facing' configuration, Fig. 6a. In this configuration, no Pd K shell X-rays would have been observed. Furthermore, the cathode was a 1 mm thick plate of Pd. As shown

Table 4
Estimating the Pd K shell X-ray peak area resulting from the passage of 1.7 MeV protons, 11 MeV alphas, and 16 MeV alphas that were identified by Lipson et al. [7].

Particle and energy	5.3 MeV α	1.7 MeV p	11 MeV α	16 MeV α
Range in Pd (μm)	9.76	13.11	28.49	55.7
Ratio[a]	N/A	1.34	2.92	5.71
Number of particles	3700	9.6×10^{-4} [7]	57.2×10^{-4} [7]	57.2×10^{-4} [7]
Equivalent number of 5.3 MeV α particles[b]	N/A	12.9×10^{-4}	167×10^{-4}	326.6×10^{-4}
Peak area[c]	1.163×10^{-4}	4.05×10^{-11}	5.24×10^{-10}	1.03×10^{-9}

[a] Ratio = [range of 1.7 MeV p or 11, 16 MeV α]/[range of 5.3 MeV α].
[b] Equivalent = [number of 1.7 MeV p or 11, 16 MeV α] × ratio.
[c] Peak area of the 3700 5.3 MeV α particles was measured to be 1.163×10^{-4}. This correlation was used to estimate the expected Pd K shell X-ray peak areas resulting for the passage of 1.7 MeV protons, 11 MeV alphas, and 16 MeV alphas through the Pd lattice.

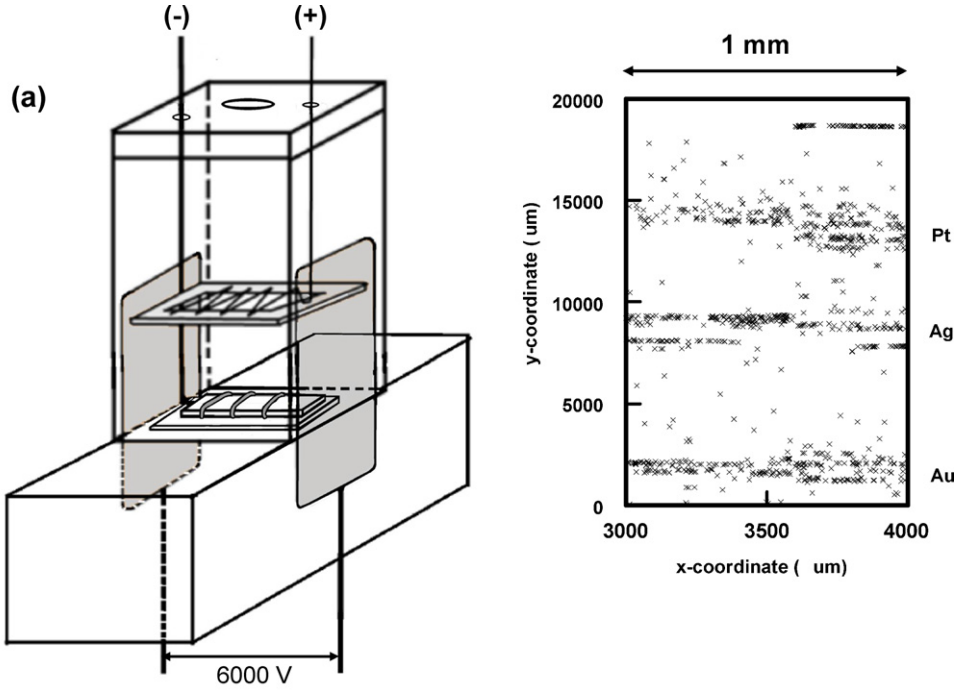

Fig. 10. (a) Schematic of a cell used in an E-field experiment. The cathode is composed of a Pt, Ag, and Au wires connected in series. The external voltage applied is 6000 V DC with a 6% AC ripple. (b) Spatial distribution of positively identified tracks obtained by scanning a 1 mm × 20 mm area on a CR-39 detector used in a Pd/D co-deposition experiment done in the presence of an external E-field. Total number of positively identified tracks is 1079. Placement of the Pt, Ag, and Au wires is indicated.

by the plot in Fig. 8a, self-absorption of the Pd K shell X-rays would also have been an issue.

The Pd/D co-deposition experiments of Mosier-Boss et al. [9–11] typically ran for two weeks. Fig. 10a shows the experimental configuration used in an experiment in which an external 6000 V DC (with a 6% AC ripple) electric field was applied across the cell after the Pd had been plated out. The 6% AC component allows coupling of the electric field into the cathode. In this particular experiment, Pt, Ag, and Au wires were connected in series, over the CR-39 detector, as shown in Fig. 10a. The detector used in this experiment was scanned using an automated scanning track analysis system to obtain quantitative information on the pits produced in the CR-39. The system has a high quality microscope optical system (Nikon cfi series) operating at a magnification high enough to discriminate between tracks and background. Fig. 10b shows the spatial orientation of positively identified tracks in the CR-39 detector used in the three wire experiment. It can be seen that track density correlates with the placement of the wires.

Fig. 11a shows a microphotograph of tracks in the CR-39 detector taken by the scanner. Each image taken by the scanner is then analyzed by the proprietary software of the scanner. In Fig. 11b, each numbered rectangle represents an object in the detector identified by the computer. The computer algorithm then makes 15 characteristic measurements of each object located in the image to provide reliable discrimination between etched tracks and background features present on or in the plastic detectors. These measurements include track length and diameter, optical density (average image contrast) and image symmetry. Based upon the measured properties of a feature, the computer algorithm of the automated scanning system determines whether or not the measured features are consistent with that of an energetic particle. The software algorithms ignore overlapping tracks. Fig. 11c summarizes the results of this analysis. The light colored rectangles are positively identified tracks.

The area of the CR-39 detector scanned in Fig. 10b is 1 mm × 20 mm. The total number of tracks positively identified by the scanner in this area was 1079. To determine whether or not Pd K shell X-rays would have been observed in the experiment, it is assumed that the observed tracks are due to charged particle interactions with the detector and not neutrons. As shown in Fig. 11c, the number of tracks in this one image is undercounted by a factor of ~3. Since the total area of the detector is 10 mm × 20 mm, at a minimum, the number of tracks is undercounted by a factor of 30. However, the charged particle stimulation of the Pd K shell X-rays will occur throughout the Pd deposit. Ignoring absorption of the Pd K-shell X-rays by the Pd deposit and cell components, in the worse-case scenario, it is estimated that the charged particles are undercounted by a factor of 1000. The total area of the detector is 10 mm × 20 mm. Taking this larger detector area into account, the charged particles are estimated to be undercounted by a factor of 10,000. Therefore, in this worst case scenario, the number of charged particles is 1.079×10^7. For a two week experiment (1.2096×10^6 s), the rate of particle production is estimated to be 8.9 particles s^{-1}. The 0.1 μCi ^{210}Po α source decays at a rate

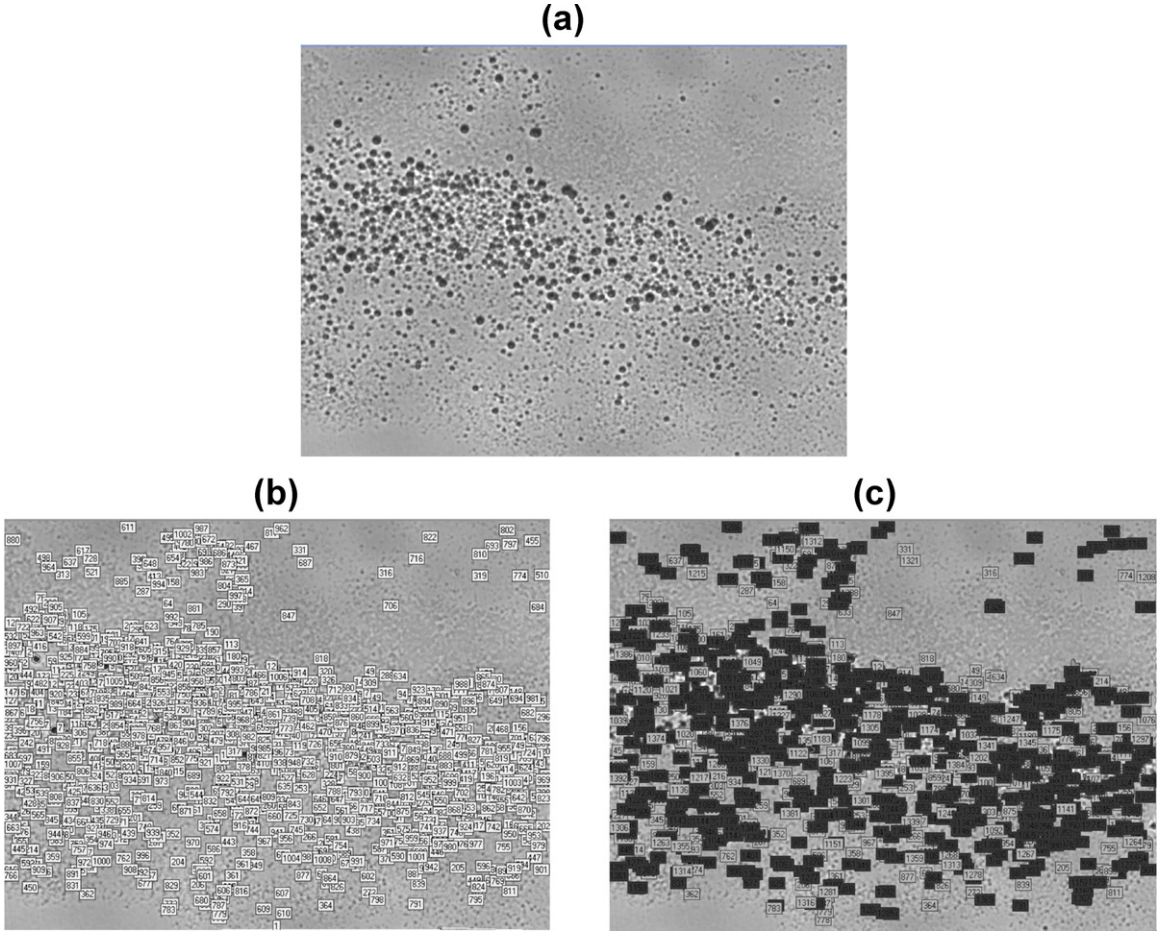

Fig. 11. (a) Photomicrograph of tracks observed in a CR-39 detector used in a Pd/D co-deposition experiment. The photomicrograph was obtained using the automated system at a magnification is 200×. (b) The image shown in (a) after undergoing computer processing and objects have been identified and numbered. These objects are indicated by the light colored rectangles. (c) Based upon measurements of object symmetry and contrast, the computer algorithm identifies tracks whose properties are consistent with those of nuclear generated tracks. These tracks are indicated by the light colored rectangles.

of 3700 particles s^{-1}. As summarized in Table 3, the calculated peak area due to the stimulation of the Pd K shell X-rays by 3700 α particles, in the time normalized spectrum, is 1.163×10^{-4}. The increase in peak area of 8.9 charged particles, in the time normalized spectrum, is calculated to be 2.9×10^{-7}. This is too small an increase in peak area to see in the measured spectrum. In addition, the experimental configuration for the E-field experiment is equivalent to the 'not-facing' configuration, Fig. 6a. In this configuration, no Pd K shell X-rays would have been observed.

4. Conclusions

In this communication, the apparent discrepancy between charged particle detection in the Pd/D system using CR-39 detectors and measurement of Pd K-shell X-rays was examined. CR-39 detectors are constantly integrating detectors, which means that once an event occurs, it is permanently stamped in the plastic. Using CR-39 detectors, Li et al. [1,3], Lipson et al. [4,7], Oriani and Fisher [6], and Mosier-Boss et al. [9–11] have reported the observation of charged particle emissions in the Pd/D systems by both gas and electrolytic loading. In contrast to CR-39, the measurement of Pd K shell X-rays is done in real time. No Pd K shell X-rays above background were observed by either Bennington et al. [20] or Deakin et al. [21] in their electrolytic loading of Pd with deuterium.

In this investigation, Pd K shell X-rays were stimulated when a thin Pd foil was placed in contact with a ^{241}Am source. However, it was found that the ^{241}Am gamma ray at 59.54 keV, and not the alpha emissions, was primarily responsible for the stimulation of the Pd K shell X-rays. These results emphasize the need to properly characterize RAM sources when doing calibrations. This was particularly borne out when conducting experiments using a ^{210}Po source, which was supposed to be a pure alpha emitter. Measurements of the ^{210}Po source, using the HPGe detector, showed the presence of three weak gamma-/X-ray lines attributed to unknown contaminant(s). However, use of this source in these experiments made it possible to separate and quantify the alpha/gamma contributions in stimulating the Pd K-shell X-rays.

Using the 0.1 μCi ^{210}Po source, it was found that the orientation of the source relative to the HPGe detector head determined whether or not the Pd K-shell X-rays would be observed. The Pd K-shell X-rays were observed when the ^{210}Po source was directly facing the detector head. No Pd K-shell X-rays were seen when the ^{210}Po source was perpendicular to, or 'not-facing,' the HPGe detector head. Consequently, no Pd K-shell X-rays would have been detected in the electrolysis experiments done by Oriani and Fisher [6], Lipson et al. [7,8], and Mosier-Boss et al. [9–11]. In addition, it was found that, although tracks significantly above background were observed in CR-39 detectors used in gas and electrolytic loading experiments, the rate of charged particle production was too low to be detected by the Pd K shell X-ray emissions.

Acknowledgements

This work was funded by the Defense Threat Reduction Agency (DTRA), and JWK Corporation. The authors would like to thank Dr. Gary Phillips, nuclear physicist, retired from the Naval Research Laboratory, US Navy, Radiation Effects Branch and Dr. Peter Hagelstein, theoretical physicist at the Massachusetts Institute of Technology, for valuable discussions on CR-39.

References

[1] X.-Z. Li, D.-W. Mo, L. Zhang, S.-C. Wang, T.-S. Kang, S.J. Liu, J. Wang, Anomalous nuclear phenomena and solid state nuclear track detector, Nuclear Tracks and Radiation Measurements 22 (1993) 599.
[2] P.B. Price, S.W. Barwick, W.T. Williams, J.D. Porter, Search for energetic-charged-particle emission from deuterated Ti and Pd foils, Physical Review Letters 63 (1989) 1926.
[3] X.-Z. Li, S. Dong, K. Wang, Y. Fang, L. Chang, C. Luo, R. Hu, P. Zhou, D. Mo, Y. Zhu, C. Song, Y. Chen, M. Yao, C. Ren, Q. Chen, The precursor of cold fusion phenomenon in deuterium/solid systems, in: Anomalous Nuclear Effects in Deuterium/Solid Systems, American Institute of Physics, New York, 1990.
[4] A. Lipson, F. Lyakhov, A. Roussetski, T. Akimoto, N. Asami, R. Shimada, S. Miyashita, A. Takahashi, Evidence for low-intensity D-D reaction as a result of exothermic deuterium desorption from Au/Pd/PdO:D heterostructure, Fusion Science and Technology 38 (2000) 238.
[5] A.S. Roussetski, Application of CR-39 plastic track detector for detection of DD and DT-reaction products in cold fusion experiments, in: 8th International Conference on Cold Fusion, Italian Physical Society, Bologna, Italy, 2000.
[6] R.A. Oriani, J.C. Fisher, Generation of nuclear tracks during electrolysis, Japanese Journal of Applied Physics 41 (2002) 6180.
[7] A.G. Lipson, A.S. Roussetski, G.H. Miley, E.I. Saunin, Phenomenon of an energetic charged particle emission from hydrogen/deuterium loaded metals, in: 10th International Conference on Cold Fusion, Cambridge, MA, 2003.
[8] A.G. Lipson, A.S. Roussetski, G.H. Miley, C.H. Castano, In-situ charged particles and X-ray detection in Pd thin film-cathodes during electrolysis in Li_2SO_4/H_2O, in: 9th International Conference on Cold Fusion, Condensed Matter Nuclear Science, Tsinghua University Press, Beijing, China, 2002.
[9] P.A. Mosier-Boss, S. Szpak, F.E. Gordon, L.P.G. Forsley, Use of CR-39 in Pd/D co-deposition experiments, European Physical Journal – Applied Physics 40 (2007) 293.
[10] P.A. Mosier-Boss, S. Szpak, F.E. Gordon, L.P.G. Forsley, Characterization of tracks in CR-39 detectors obtained as a result od Pd/D co-deposition, European Physical Journal – Applied Physics 46 (2009) 30901.
[11] P.A. Mosier-Boss, S. Szpak, F.E. Gordon, L.P.G. Forsley, Detection of energetic particles and neutrons emitted during Pd/D co-deposition, in: Low-Energy Nuclear Reactions Sourcebook, American Chemical Society, Washington, DC, 2008.
[12] K. Oda, M. Ito, H. Miyake, M. Michijima, Track formation in CR-39 detector exposed to D-T neutrons, Nuclear Instruments and Methods in Physical Research B35 (1988) 50.
[13] P.A. Mosier-Boss, S. Szpak, F.E. Gordon, L.P.G. Forsley, Triple tracks in CR-39 as a result of Pd/D co-deposition: evidence of energetic neutrons, Naturwissenschaften 96 (2009) 135.
[14] P.A. Mosier-Boss, J.Y. Dea, L.P.G. Forsley, M.S. Morey, J.R. Tinsley, J.P. Hurley, F.E. Gordon, Comparison of Pd/D co-deposition and DT neutron generated triple tracks observed in CR-39 detectors, European Physical Journal – Applied Physics 51 (2010) 20901.
[15] A.G. Lipson, A.S. Roussetski, E.I. Saunin, F. Tanzella, B. Earle, M. McKubre, Analysis of the CR-39 detectors from SRI's SPAWAR/Galileo type electrolysis experiments #7 and #5: signature of possible neutron emission, in: 8th International Workshop on Anomalies in Hydrogen/Deuterium Loaded Metals, The International Society for Condensed Matter Nuclear Science, 2008.
[16] A.K. Pandeym, R.C. Sharma, P.C. Kalsi, R.H. Iyer, Measurement of alpha to fission branching ratios of heavy actinides by sequential etching of alpha and fission tracks in CR-39, Nuclear Instruments and Methods in Physical Research B 82 (1993) 151.
[17] D. Paul, D. Ghose, R.C. Sastri, An SSNTD study of spontaneous fission fragments from the soil-gas samples of Bakreswar thermal springs, Radiation Measurements 33 (2001) 167.
[18] M. Luszik-Bhadra, F. d'Errico, L. Lusini, B. Wiegel, Microdosimetric investigations in a proton therapy beam with sequentially etched CR-39 track detectors, Radiation Protection Dosimetry 66 (1996) 353.
[19] M. Fromm, F. Membrey, A. El Rahamany, A. Chambaudet, Principle of light ions micromapping and dosimetry using a CR-39 polymeric detector: modelized and experimental uncertainties, Nuclear Tracks and Radiation Measurements 21 (1993) 357.
[20] S.M. Bennington, R.S. Sokhi, P.R. Stonadge, D.K. Ross, M.J. Benham, T.D. Beynon, P. Whithey, I.R. Harris, J.P.G. Farr, A search for the emission of x-rays from electrolytically charged palladium-deuterium, Electrochimica Acta 34 (1989) 1323.
[21] M.R. Deakin, J.D. Fox, K.W. Kemper, E.G. Myers, W.N. Shelton, J.G. Skofronick, Search for cold fusion using X-ray detection, Physical Review C 40 (1989) R1851.
[22] J.F. Ziegler, J.P. Biersack, The Stopping and Range of Ions in Solids, Pergamon, New York, 1985.
[23] http://ie.lbl.gov/toi/nuclide.asp?iZA=950241
[24] D. Nikezic, K.N. Yu, Formation and growth of tracks in nuclear track materials, Materials Science and Engineering R 46 (2004) 51.
[25] http://sales.hamamatsu.com/en/products/electron-tube-division/x-ray-products/scintillators.php
[26] http://www.ehow.com/how_7630142_calculate-xray-absorption.html
[27] E.M. Gullikson, Mass absorption coefficients, in: X-ray Data Booklet, Lawrence Berkeley National Laboratory, Berkeley, CA, 2001.
[28] http://henke.lbl.gov/optical_constants/pert_form.html
[29] http://web-docs.gsi.de/~stoe_exp/web_programs/x_ray_absorption/index.php